# Coordinated Control of DC Circuit Breakers in Multilink HVDC Grid

Xibei Zhao, Jianzhong Xu, *Senior Member, IEEE,* Gen Li, *Member, IEEE,* Jinsha Yuan, Jun Liang, *Senior Member, IEEE,* and Chongru Liu, *Senior Member, IEEE,*

***Abstract* — High voltage DC grid is developing towards more terminals and larger transmission capacity, thus the requirements for DC circuit breakers (DCCB) will rise. The conventional methods only use the faulty line DCCB to withstand the fault stress, while this paper presents a coordination method of multiple DCCBs to protect the system. As many adjacent DCCBs are tripped to interrupt the fault current, the fault energy is shared, and the requirement for the faulty line DCCB is reduced. Moreover, the adjacent DCCBs are actively controlled to help system recovery. The primary protection, backup protection, and reclosing logic of multiple DCCB are studied. Simulation confirms that the proposed control reduces the energy dissipation requirement of faulty line DCCB by around 30-42 %, the required current rating for IGBTs is reduced, and the system recovery time reduced by 20-40 ms.**

***Index Terms*—DC circuit breakers (DCCB), DC grid, DC protection, DC fault, fault current limiting.**

## I. Introduction

HIGH voltage DC grid is a promising solution for large scale renewable energy transmission and regional AC grid interconnection. A multilink DC grid is built with several transmission lines linked to one DC bus, which can improve functionality, stability, and reliability of the power grid while decreasing the investment cost of many two-terminal DC projects [1-2]. DC grid is characterized by low impedance and thus a major challenge of the DC grid is the fast propagation of DC fault [3-4]. However, a multilink of transmission lines will further aggravate this challenge.

To meet the requirements of DC grid protection, the fault current should be interrupted within few milliseconds. A hybrid DC circuit breaker (DCCB), which can achieve low power loss and fast fault interruption at the same time, is considered as an effective solution for DC grid protection. The DCCB has better technical performance as it only isolates the faulty line, but other converter-based fault interruption methods need the near fault converter participate in the fault clearing, therefore, the fault area expand [5-9]. The concept of hybrid DCCB was proposed in [10], and verified by a prototype with 10 kA/2 ms fault interruption capability. State Grid Cooperation of China installed the first practical installation of hybrid DCCB in Zhoushan 200 kV five-terminal DC project with a 15 kA/3 ms interruption capacity [11]. In 2020, the 25 kA/3 ms hybrid DCCB will be used in Zhangbei 500 kV DC grid [12].

Being one of the disadvantages, hybrid DCCBs will increase the investment and operational costs when a large number of DCCBs are installed at each terminal of all the transmission lines in a multilink DC grid. To address this issue, one feasible approach is to reduce the cost of individual DCCBs, and simplified topologies and improved control algorithms are proposed [13]. A diode bridge-type rectifier is used to regulate bidirectional current to unidirectional current, thus no need for the IGBT units with bidirectional fault blocking capability [14, 15]. Using some auxiliary capacitors, the Thyristors can be used to replace the IGBTs for cheaper prices [16, 17]. By sequential triggering subunits within hybrid DCCB, the peak fault current and energy dissipation are reduced by an earlier blocking of the subunits [18, 19], thus increasing the controllability of the hybrid DCCB topologies.

Another approach is to reduce the required numbers of DCCB. In this category, the integrated DCCB can be installed at each DC bus rather than using several line-side DCCBs [20]. The integrated DCCB will share the use of semiconductor devices, so a special designed circuit is needed to ensure that the fault current from any direction flows into the forward direction of the IGBTs [21, 22]. In [23], each normal current branch of the DCCB is switched off to act as a rectifier, and the remaining branch will commutate the fault current to IGBTs.

The above two approaches both use one DCCB to deal with one primary protection, the individual DCCBs have the benefit of simple fault interruption logic while the integrated DCCBs cost less due to the reduced installation number. However, the fault voltage and current stresses will be fully imposed on the one integrated or individual DCCB, and the stresses will rise when the links connected to the same bus increase.

In this study, a coordination method of multiple DCCBs to protect one faulty line is proposed. Since the fault energy feeding from the adjacent lines will rise in multilink DC grid, the DCCBs in adjacent lines also participate the protection of the faulty line. Thus, the fault energy is shared by multiple DCCBs, and the requirement for faulty line DCCB will be reduced. Moreover, by using the current-limiting control DCCB, the current on the adjacent lines are actively controlled, which can help to accelerate the power recovery process of the DC grid.

Compared to the existing approach of one DCCB installed on one line, the proposed method can be used to upgrade the protection performance of the existing grid. Compared to the integrated DCCB, the proposed scheme doesn't rely on a

This work was supported by National Key R&D Program of China (2018YFB0904600) and the National Natural Science Foundation of China under grant 51777072.

X. Zhao, J. Xu, J. Yuan and C. Liu are with the State Key Laboratory of Alternate Electrical Power System with Renewable Energy Sources, North China Electric Power University (NCEPU), Beijing, China.

J. Liang is with the School of Engineering, Cardiff University, UK

Corresponding author: J. Xu (xujianzhong@ncepu.edu.cn). J. Liang (LiangJ1@cardiff.ac.uk)

complex current commutation process during the fault, and the backup protection can still be achieved by the adjacent DCCBs.

Following the Introduction, the control modes of DCCB is introduced in Section II. The coordination control for the multiple DCCBs on different lines is proposed in Section III, which considers primary/backup protection, fault reclosing and fast recovery. In Section IV, the proposed method is validated in HVDC grids simulation. The comparison and discussion is given in Section V, and Section VI concludes this paper.

## II. The Control Modes of DCCB

The conventional control of DCCB switches all IGBT units of its main breaker (MB) synchronously, while the sequential blocking control and current limiting control of DCCB switch its MB IGBT units separately. A test circuit of 500 kV/2 kA hybrid DCCB model is shown in Fig. 1 to illustrate the DCCB's performance under three control modes.

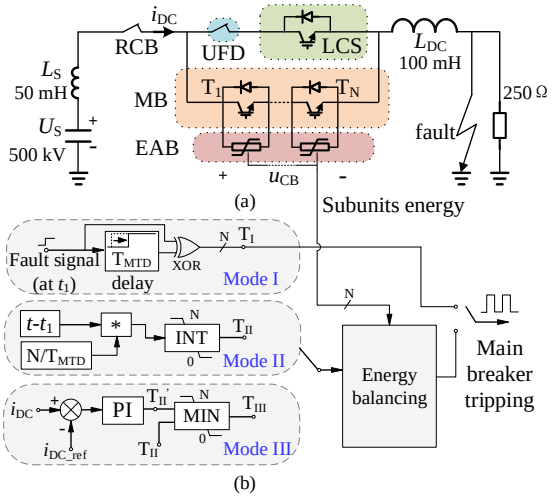


Fig. 1. DCCB text scheme. (a) Test circuit; (b) DCCB control modes.

In Fig. 1, $U_S$ and $L_S$ represent the converter system DC voltage and its equivalent inductance. $L_{DC}$ represents the lineside DC inductance, RCB represents the residual circuit breaker. The DCCB consists of an ultra-fast disconnector (UFD), a load commutation switch (LCS), a main breaker (MB) with N (=8) subunits, and an energy absorption branch (EAB) build up with metal-oxide varistors. The three different control strategies of main breaker are drawn in Fig. 1 (b):

① Mode I (conventional DCCB): All the MB subunits share the same triggering signal $T_I$, they will be conducted after receiving the fault signal at $t_1$, and blocked when the UFD successfully separated after the mechanical time delay ($T_{MTD}$). This is achieved by XORing the step fault signal and its delay.

② Mode II (sequential blocking DCCB) [18, 19]: $T_{II}$ is the number of blocked subunits which is calculated by evaluating the contact insulation voltage of the UFD, then round down through the limiter. In this mode, a proportion of the subunits are blocked sequentially during the UFD separation, and all the subunits are blocked after the UFD fully opened at $t_2$.

③ Mode III (sequential current-limiting DCCB) [24]: A current feedback control is employed to control the DC current by changing the number of inserted varistors, where, $i_{DC\_ref}$ is the reference DC current and $i_{DC}$ is the real-time measured current. Signal $T_{II}$ is used to limit the blocked number of subunits during the UFD separation, and $T_{II}'$ is required number of subunits generated from the current controller. At last, the number of blocked subunits $T_{III}$ is determined by the minimum value of $T_{II}$ and $T_{II}'$.

An energy balancing module is used in the mode II and III to ensure that all the subunits equally share the fault energy [24] the control frequency is 10k Hz [19]. The dissipated energy of each subunit is calculated by its corresponding sensor, and the energy balancing module determines the x subunits with the lowest energy are blocked.

Among the three modes, Mode I is the very basic control of DCCB, which considers all subunits as an entity, and the control signal comes from an open loop signal. The Mode II can control each subunit independently, but $T_{II}$ also comes from an open loop. Mode III further adopts close loop control, so it has the highest flexibility. Moreover, Mode II and III can be seen as Mode I step by step upgrade through software and hardware. The DCCB's performance of three modes are shown in Fig. 2.

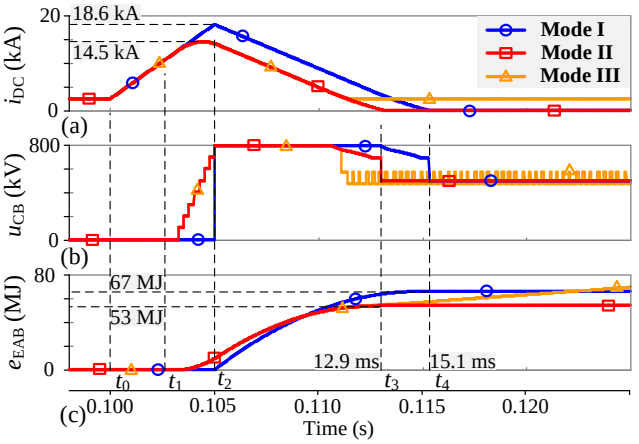


Fig. 2. DCCB performance. (a) DC current; (b) DC breaker voltage; (c) Energy dissipated in the EAB.

The fault is applied at $t_0$, and detected at $t_1$. As shown in Fig.2 (a), the peak current of Mode I is 18.6 kA, while the peak current of Mode II and III reduced to 14.5 kA. It is seen from Fig. 2 (b) that the breaker voltage of Mode I is established suddenly after UFD fully opened at $t_2$, but Mode II and III can partly insert subunits during UFD separation. Moreover, the energy dissipation is reduced from 67 MJ to 53 MJ due to the earlier blocking of subunits in mode II, see Fig. 2 (c). Mode III has the same response as mode II in the beginning, then the subunits are controlled on/off to follow the $i_{DC\_ref}$ (=2 kA). Note that the energy dissipation in mode III will continuously increase, which indicates that the dissipated energy will increase if Mode III is applied to the faulty line DCCB. However, it can be applied to the adjacent DCCBs as its fault energy is lower than the faulty line. Base on the different control modes, the coordination methods between DCCBs can be discussed.

## III. Coordination Method of DCCBs in DC Grid

In this section, the coordination methods of Mode II&III are investigated, in which the primary/backup protection, fault reclosing and fast recovery are considered.

### A. Coordination Method for Primary Protection

The sequential blocking of DCCB can reduce the peak fault current and fault energy by controlling each subunit independently, and the dissipation energy can be reduced by the coordination control at the same time. The schematic diagram of the proposed coordination method is shown in Fig. 3. In which, a three-link DC bus is assumed and the MMC0 is the converter directly connected to the faulty line, MMC1&2 are remote converters feeding fault currents through DC lines.

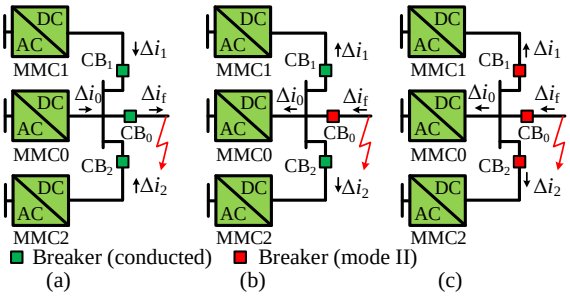


Fig. 3. Coordination method for sequential blocking DCCBs. (a) Current trend after fault; (b) conventional protection; (c) the proposed coordination protection

After the fault occurs, all the converters in the DC grid have a trend to feed fault current into the fault point. As shown in Fig.3 (a), the current from the MMC0 will be the main part of the total fault current because it has less inductance on the fault path, while the proportion will decrease with more DC links. However, the peak fault current will increase with more DC links, and the energy dissipation requirements of the DCCBs will increase faster since more inductive energies stored in the DC links have to be dissipated (this will be validated later in Section IV).

The conventional protection only uses one $CB_0$ (mode II) to interrupt the fault current, and the current on the adjacent lines will decrease naturally to achieve a new steady state, see Fig. 3 (b). To reduce the requirement of faulty line CBs, the breakers installed on the adjacent lines ($CB_{1\&2}$) can also be tripped (mode II) to help $CB_0$, see Fig. 3 (c). As all corresponding CBs are in the same station, they are supposed to operate simultaneously. The adjacent CBs are designed to deal with their line fault, but the adjacent lines' currents are much smaller than the faulty line's current. Therefore, the adjacent DCCBs can easily interrupt their currents.

The equivalent circuit of DC grid fault shown in Fig. 4 is used to analyze the fault interruption performance, where all the adjacent and remote terminals are considered as constant DC voltage sources. In Fig. 4, $U_S$ and $L_S$ represent the converter DC voltage and its equivalent inductance. $L_{DC}$ represents the DC inductance, in which the label 0 means the elements on the faulty line and the directly linked converter, the label *1-n* means elements on the *n* adjacent lines.

When a DC solid fault occurs at $t_0$, detected at $t_1$, before the breaker is tripped at $t_2$, the DC bus voltage $u_{bus}$ is:

$$u_{bus} = L_{DC0}\frac{di_f}{dt} = U_{S\beta} - L_{eq\beta}\frac{di_\beta}{dt},\quad \beta \in \{0, n\} \tag{1}$$

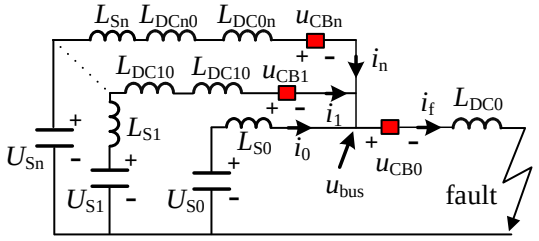


Fig. 4. Equivalent circuit for a DC grid fault.

Where, the subscript $\beta$ is {0, 1, 2, …, n} to represent the DC lines and corresponding converters. $L_{eq\beta}$ is the equivalent inductance of each line given in (2)

$$\begin{cases} L_{eq\beta} = L_{S0},\ \beta = 0 \\ L_{eq\beta} = L_{S\beta} + L_{DC\beta 0} + L_{DC0\beta},\ \beta = 1, 2, ..., n \end{cases} \tag{2}$$

The fault current will reach its maximum value if all converters can be considered to keep at the rated DC voltage ($U_S$) in a short time. Thus, the DC fault current on each line are:

$$\begin{cases} i_f = i_{f(t_0)} + \dfrac{U_S}{L_{DC0} + L_{eq}} t \\ i_\beta = i_{\beta(t_0)} + \dfrac{L_{eq}}{L_{eq\beta}} \dfrac{U_S}{L_{DC0} + L_{eq}} t \\ \dfrac{1}{L_{eq}} = \sum \dfrac{1}{L_{eq\beta}} \\ t \in (t_0, t_2),\ \beta \in \{0, 1, ..., n\} \end{cases} \tag{3}$$

The $L_{eq}$ will become smaller with more DC links, and the rising speed of $i_f$ will increase, but it will have a maximum value when $L_{eq}$ equals zero. The rising rate of $i_\beta$ is inversely proportional to the value of $L_{eq\beta}$.

If one DCCB based on sequential control is used to interrupt the faulty line, the subunits of DCCB are blocked during the UFD separation process. Before the UFD is fully separated, the $u_{CB}$ can be seen to follow the isolation voltage of UFD. After the UFD fully separated, the CB's voltage will reach its rating voltage $U_{CB}$ [15]. Thus, the voltage across the DCCB is:

$$u_{CB} = \begin{cases} K \times t,\ t \in (t_1, t_2) \\ U_{CB},\ t \in (t_2, t_3) \end{cases} \tag{4}$$

During $t_1$-$t_2$, the fault current changes with the growth of $u_{CB}$:

$$\begin{aligned} i_f &= i_f(t_1) + \int_{t_1}^{t} \frac{U_S - u_{CB}}{L_{DC0} + L_{eq}} dt \\ &= i_f(t_1) + \frac{U_S(t - t_1) - 0.5K(t - t_1)^2}{L_{DC0} + L_{eq}},\ t \in (t_1, t_2) \end{aligned} \tag{5}$$

Due to the earlier blocking of subunits than the conventional DCCB, the peak fault current is limited, and the fault current will achieve its max value when the breaker voltage equals the DC system voltage.

$$i_{f\_peak}=i_f(t_1)+\frac{U_S\frac{U_{CB}}{K}-0.5K(\frac{U_{CB}}{K})^2}{L_{DC0}+L_{eq}} \tag{6}$$

After all the subunits are blocked at $t_2$, the fault current decreases as:

$$i_f=i_f(t_2)+\frac{U_S\text{-}u_{CB0}}{L_{DC0}+L_{eq}}t,\ t\in(t_2,t_3) \tag{7}$$

The dissipation energy is the sum energy during $t_1$-$t_3$:

$$\begin{aligned}E_{CB}&=\int_{t_1}^{t_2}i_{f(t_2\text{-}t_1)}Ktdt+\int_{t_2}^{t_3}i_{f(t_3\text{-}t_2)}U_{CB}dt\\&=0.5i_{f(t_1)}K(t_2\text{-}t_1)^2+\frac{\frac{1}{3}UsK(t_2\text{-}t_1)^3-\frac{1}{8}k^2(t_2\text{-}t_1)^4}{L_{DC0}+L_{eq}}\\&+U_{CB}i^2_{f(t_2)}\frac{L_{DC0}+L_{eq}}{2(U_{CB}\text{-}U_S)}\end{aligned} \tag{8}$$

The proposed coordination method of multiple DCCBs will bring new characteristics if multiple DCCBs are used to interrupt the fault. The faulty line current will reduce faster due to the participation of the adjacent DCCBs. Assuming all the DCCBs are tripped, the DCCBs on the adjacent lines will also tripped to accelerate the fault current decay speed. The DC bus voltage is:

$$\begin{aligned}u_{bus}&=L_{DC0}\frac{di_f}{dt}+u_{CB0}=U_S\text{-}L_{eq\beta}\frac{di_\beta}{dt}-u_{CB\beta}\\&=U_S\text{-}L_{S0}\frac{di_0}{dt},\ \beta\in\{1,2,...,n\}\end{aligned} \tag{9}$$

Considering the fact that each DCCB will block its subunits simultaneously, the fault current under the coordination method of mode II is

$$\begin{aligned}i_f&=i_f(t_1)+\int_{t_1}^{t}\frac{U_S-\frac{(2n+1)}{n+1}Kt}{(L_{DC0}+\frac{1}{n+1}L_{eq})}dt\\&=i_f(t_1)+\frac{U_St-0.5\frac{(2n+1)}{n+1}Kt^2}{(L_{DC0}+\frac{1}{n+1}L_{eq})},\ t\in(t_1,t_2)\end{aligned} \tag{10}$$

Equation (10) shows that the decay speed of the fault current will be faster with more adjacent DCCBs participating in the fault interruption process. Furthermore, the energy dissipation on the faulty line DCCB is reduced due to a faster fault current decay speed. The peak fault current is also reduced to:

$$i_{f\_peak}=i_f(t_1)+\frac{Us\frac{U_{CB}}{K}-0.5\frac{(2n+1)}{n+1}K\left(\frac{U_{CB}}{K}\right)^2}{(L_{DC0}+\frac{1}{n+1}L_{eq})} \tag{11}$$

The energy dissipation requirement for the faulty line DCCB can be calculated as:

$$\begin{aligned}E_{CB}&=0.5i_f(t_1)\times K(t_2\text{-}t_1)^2\\&+\frac{\frac{1}{3}UsK(t_2\text{-}t_1)^3-\frac{1}{8}\frac{2n+1}{n+1}K^2(t_2\text{-}t_1)^4}{L_{DC0}+\frac{1}{n+1}L_{eq}}\\&+U_{CB}\times i_f^2(t_2)\times\frac{L_{DC0}+L_{eq}}{2\frac{2n+1}{n+1}(U_{CB}\text{-}U_S)}\end{aligned} \tag{12}$$

Comparing equation (12) to (8), the second and third part of equation (12) becomes smaller with the growth of $n$. Therefore, the faulty line DCCB energy dissipation is reduced. Note that if no adjacent lines exist (n=0), equations (10) and (12) are the same as equations (5) and (8), respectively.

Although the breaking of all adjacent DCCBs can help maximum share the fault energy from $CB_0$, a totally breaking will damage the DC grid connection. Therefore, $CB_{1\&2}$ is designed to operate in the current limiting mode to balance the energy sharing and system connection requirements.

### *B. Coordination Method for Assisting the System Fast Recovery and Backup Protection*

The sequential current limiting DCCB (Mode III) can applied to the adjacent lines. It is known that the fast system recovery is also important for the HVDC grid after the fault clearance, and the sequential current limiting DCCB can also contribute to this process in two ways:

① Demagnetize the adjacent lines: As the fault current is much higher than the steady state current, the adjacent DCCBs action can assist current decreasing in the proposed coordination method. The excess line reactor energy is demagnetized by the DCCBs, so that the current of adjacent lines is actively reduced to a steady state value. However, this is not the case for the single DCCB protection since its power flow can only be established naturally.

② Limit the current fluctuation during recovery process: The $CB_{1\&2}$ operate in mode III, then the circuit breaker will limit its current not over the post-fault steady current. The $i_{DC\_ref}$ of current limiting mode can be obtained from the steady state power flow calculation [25], then the system fluctuation is forcibly suppressed by the circuit breaker. As shown in Fig. 5 (a), the $CB_0$ operates in mode II, and $CB_{1\&2}$ operate in mode III. After the system recovered, the $CB_{1\&2}$ will switch to the pre-fault state.

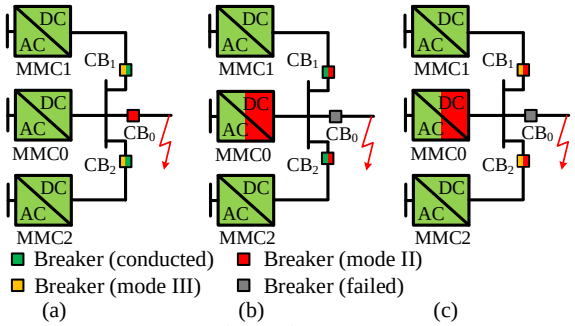


Fig. 5. Coordination method for (a) fast recovery; (b) conventional backup protection; (c) the proposed backup protection

Based on the proposed primary protection method, the backup protection of multiple DCCBs are different from the conventional scheme. The conventional backup protection will only be tripped after receiving the fault signal of the faulty line DCCB, then the near fault converter (MMC0) and adjacent DCCBs ($CB_{1\&2}$) are blocked, as shown in Fig. 5 (b). The backup protection of coordination control only has a little difference to the main protection. All the breakers will switch to mode II after receiving the signal of $CB_0$, and the near fault converter will be blocked at the same time, see Fig. 5 (c). The converter will not be blocked and only the faulty line will be isolated if the DCCBs operate successfully, so no converter is lost in the proposed method, which is critical for a fully selective protection. Although the adjacent DCCBs are activated, they are used to actively help the power flow rebalance. Therefore, the selectivity of the proposed method is still guaranteed.

The sequence of the proposed coordination control is shown in Fig. 6. The $CB_0$ is blocked to isolate the faulty line once the fault is detected. $CB_{1\&2}$ are used to regulate the currents in the adjacent lines within the threshold. If $CB_0$ fails, the system will switch into the backup protection. Then, MMC0 and $CB_{1\&2}$ will be blocked. The difference between the proposed method and conventional DCCB protection is highlighted in grey in Fig. 6, which shows the adjacent DCCBs ($CB_1$ and $CB_2$) will operate in the current-limiting mode to limit adjacent lines' current fluctuation. As the proposed coordination method only has one additional operation, its complexity is only slightly increased with acceptable reliability and feasibility.

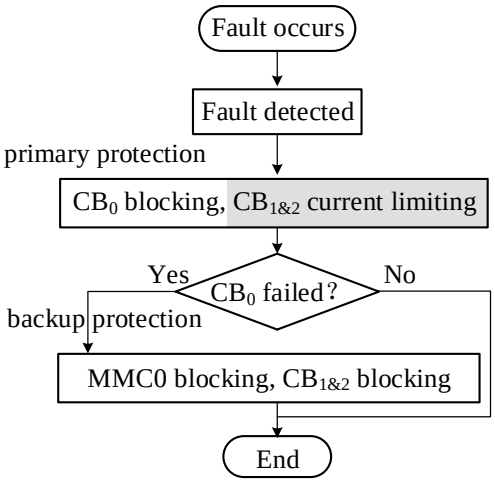


Fig. 6. Control logic of the coordination method of multiple DCCBs.

The converter will not change its state if the DCCB operation properly, thus the protection is achieved by the DCCBs. If the faulty line DCCB is failed, the converter will also be blocked, but it will only happen in the backup protection. The coordination control of backup protection has no difference at the beginning of primary protection, thus no time delay waiting for the failure signal of $CB_0$. Therefore, the proposed backup protection will act faster than the conventional method. Further, this coordination method blurs the difference between primary and backup protections, the system only needs to trip all DCCBs first, then switch to system recovery or backup protection operation according to the condition of $CB_0$. Moreover, the proposed methods of multiple DCCBs can be applied to all kinds of fully controlled modular DCCBs.

### *C. Coordination Method for Reclosing Process*

The faulty line DCCB needs to reclose in 200-300 ms after a fault to distinguish permanent fault or temporary fault. The very basic reclosing method of DCCB is to totally reclose the main breaker subunits, then block all subunits again if the fault still exists, see Fig. 7 (a). In the coordination control, the faulty line DCCB ($CB_0$) will control its current after being reclosed, and the $i_{DC\_ref}$ can be chosen as the pre-fault steady current. Therefore, if the fault disappears, the DC current can keep stable without the help of DCCB. If the subunits of DCCB is still inserted to control the DC current after a certain time delay, the fault can be considered as permanent fault, then the DCCB will be permanently blocked, see Fig. 7 (b).

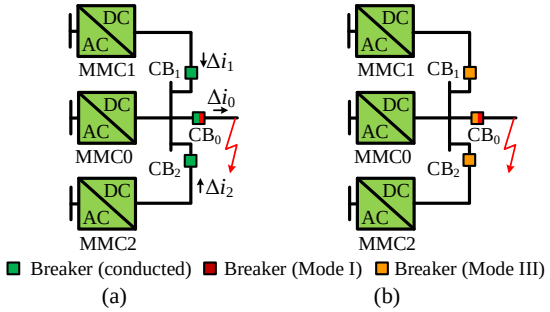


Fig.7 Reclosing scheme of (a) conventional single DCCB; (b) multiple sequential DCCBs.

The reclosing process is divided into 3 steps, and its logic is also drawn in Fig. 8.

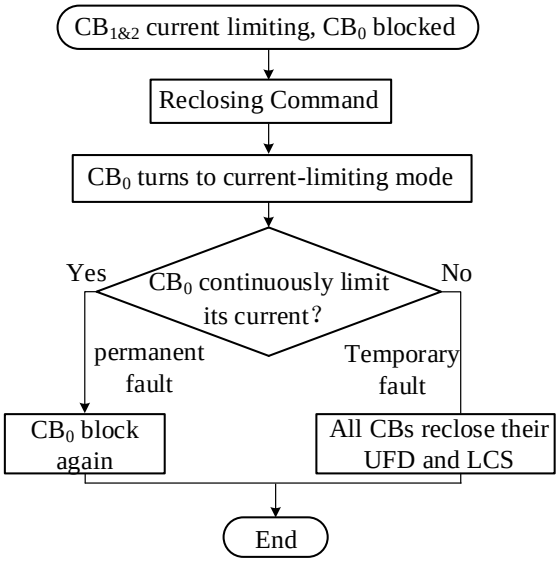


Fig. 8. Control logic of the reclosing process of multiple DCCBs.

① Before the reclosing command is received, the $CB_0$ is blocked. The $CB_{1\&2}$ continuously operate in the current-limiting mode.

② When the reclosing command is sent to $CB_0$, $CB_0$ turns to current-limiting mode. If the fault exists, the faulty line current grows rapidly, $CB_0$ will automatically limit the fault current. If the fault disappears, the power flow will

gradually be rebalanced, and the current on the faulted line will not exceed the current limitation.

③ Based on the statement of $CB_0$, $CB_0$ will block again when the fault exists, or all CBs reclose their UFDs and LCSs after fault disappears.

## IV. HVDC Grid Simulation Study

### A. Simulation System

The superiority of the proposed coordination control is validated respectively in four- and seven-terminal 500 kV DC grids, aiming to showcase the applicability of the proposed method in a multilink HVDC grid. The simulation built in PSCAD V4.6 is based on the Zhangbei HVDC grid in China [26], which is a four-terminal meshed DC grid (MMC 1&2&3&4). The additional three stations (MMC 5&6&7) are the phase II construction plan of this project, which will be built in the future.

The structure of the test system is given in Fig. 9, in which the single line diagram is used to represent a bipolar DC grid. All converters are controlled to zero reactive power, and the active power control parameters are also marked in Fig. 9. The parameters of each converter are given in the table I. At $t$ = 1 s, a solid metal pole-to-pole DC short-circuit fault is applied at the near end of MMC1, then the proposed coordination method is studied in the four- and seven-terminal DC grid.

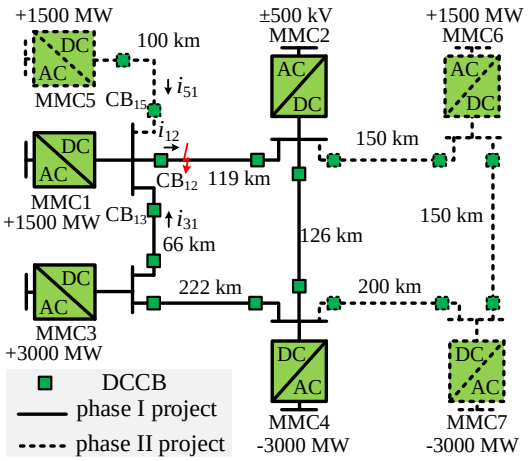


Fig. 9. Structure of the studied HVDC grid.

TABLE I
PARAMETERS OF THE DC GRID

| Items | Station1&2&5&6 | Station 3&4&7 |
|---|---|---|
| AC voltage | 230 kV | 500 kV |
| Transformer Capacity | 1700 MW | 3400 MW |
| Transformer Leakage | 0.1 pu | 0.15 pu |
| Arm Inductance | 75 mH | 100 mH |
| SM Number | 250 | 250 |
| SM Capacitance | 7500 μF | 15000 μF |
| $L_{DC}$ Inductance | 100 mH | 100 mH |

For the four-terminal DC grid (MMC 1-4), each DC bus is only linked to two transmission lines, thus two DCCBs are used to handle the DC fault. When the phase II of the project is commissioned, a seven-terminal DC grid is formed. Due to the lower impedance and higher energy storage in the seven-terminal system, the energy dissipation requirement is much higher than before. The DC bus connected to MMC 1&2&4 have 3 DC lines, then three DCCBs are used.

The studied DCCBs is the same as shown in Section II, which have 8 subunits in the simulation and each one has a peak transient voltage of 100 kV. The DC fault is set at $t$ = 1.000 s and detected at $t$ = 1.003 s. The operation delay of the UFD is set as 2 ms. As all the DCCBs are deployed in the same station, the commutation delay, which is usually less than 100 μs, is neglected. Thus, all DCCB can receive the control signal at the same time. For conventional DCCB, the $CB_{12}$ will be totally blocked at $t$ = 1.005 s, but the sequential DCCBs can start to insert their subunits from $t$ = 1.003 s.

Three cases are compared and discussed both in the four- and seven-terminal DC grid: 1) single conventional DCCB (**Sin Con CB**). 2) single sequential blocking DCCB (**Sin Seq CB**) and 3) coordination of multiple sequential DCCBs (**Mul Seq CB**). The case 3 will use sequential current limiting DCCB (Mode III) on the adjacent lines to assist the recovery of DC grid. As indicated before, the single conventional DCCB is seen as the benchmarked case for comparison. The single sequential blocking DCCB has better performance than the conventional DCCB, and the proposed coordination control of multiple DCCBs will shows a better performance than single DCCB.

### B. Coordination Protection in Four-terminal DC grid

a) *Fault interruption performance of primary protection*

The performance of coordination of sequential DCCB is drawn in Fig. 10, where the diagram of single conventional DCCB is drawn in gray line for comparison. The single sequential blocking DCCB can reduce its the peak current and fault energy, the simulation result shows the peak fault current is reduced from 15.9 kA to 12.9 kA, and the fault energy is reduced by 15.7 %, see Fig. 10 (a) and (b).

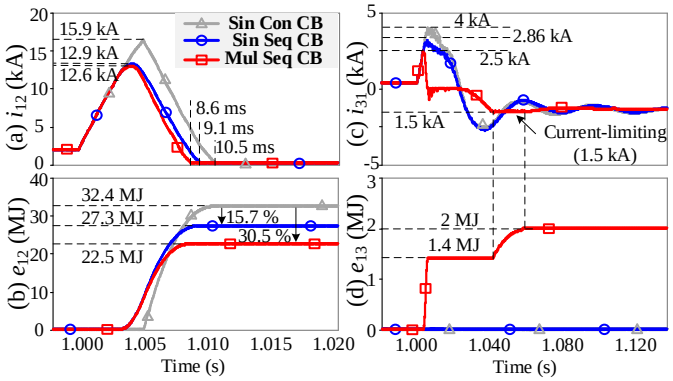


Fig. 10. Comparison of fault interruption performance of the single and multiple sequential DCCB. (a) faulty line current; (b) faulty line DCCB energy; (c) adjacent line current; (d) adjacent line DCCB energy.

The coordination control of sequential DCCBs has a significant influence on the fault energy, although the peak fault current is reduced from 12.9 kA to 12.6 kA, the fault energy is reduced by 30.5 % compared to the single conventional DCCB method. In Fig. 10 (c), the adjacent line current $i_{31}$ shows that the fault current will decrease with the assistance of $CB_{13}$, and its fluctuation is limited by the DCCB current-limiting control

during recovery process. The $e_{13}$ shows an energy dissipation of fault current interruption and current-limiting, see Fig. 10 (d).

The system recover speed is similar between the single conventional or sequential blocking DCCB, see Fig.11 (a). If multiple sequential DCCBs are used, the recovery process will be much faster. The active power of MMC1 will recovery in approximately 35 ms after fault, which is reduced around 20 ms compared to the single conventional DCCB. The capacitor voltage is also reduced from 2.6 kV to 2.36 kV, see Fig.11 (b), indicates that the proposed coordination method can result in a smaller fluctuation.

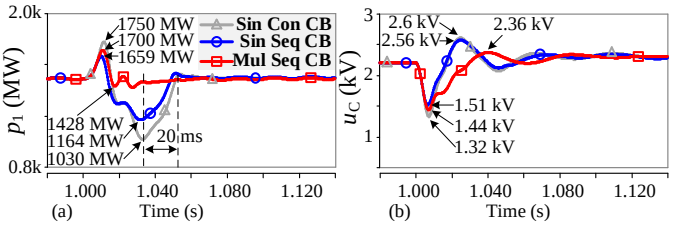


Fig. 11. Comparison of recovery process under sequential DCCB. (a) MMC1 output power; (b) MMC1 capacitor voltage.

b) *Fault interruption performance of backup protection*

The coordination control can also reduce the energy dissipation on the backup DCCB ($CB_{13}$). The $i_{31}$ and $e_{13}$ under the conventional or sequential DCCB are shown in Fig. 12. As the conventional backup protection relies on the failure signal of faulty line DCCB, thus the MMC1 is blocked at 1.005 s, and $CB_{13}$ are blocked 2 ms later. The $CB_{13}$ is blocked at 1.005 s under the coordination method of DCCBs, it will keep blocking after the failure of $CB_{12}$, and the MMC1 is blocked at 1.005 s.

The $i_{31}$ and $e_{13}$ of backup protection under single and coordination method of DCCB are shown in Fig. 12 (a) and (b). The single sequential DCCB shows a better performance in backup protection than conventional DCCB, the peak fault current and dissipated energy can be reduced by 25.4 % and 29.2%, respectively. Due to an earlier blocking of DCCB, the coordination control of DCCBs has less peak fault current, and the fault energy on $CB_{13}$ is reduced by 60.3 %, which shows a lower energy loss and faster backup fault interruption. The dissipation energy also reduced by 77.6 %, which shows the system will lose less energy in the backup protection process.

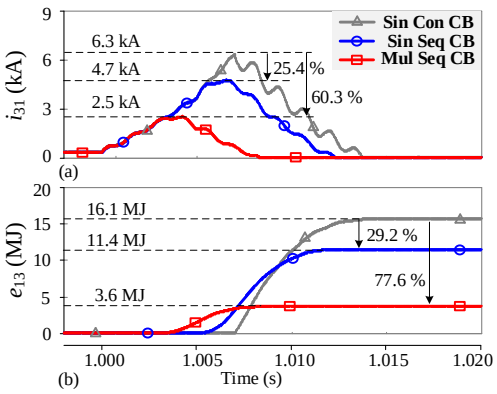


Fig. 12. Comparison of backup protection performance. (a) adjacent line current; (b) adjacent line CB's energy.

*C. Coordination Protection in Seven-terminal DC grid*

a) *Fault interruption performance of primary protection*

The performance of coordination control of sequential DCCBs is drawn in Fig. 13. The $i_{12}$ drops to zero in 9.0 ms with multiple DCCBs, and the peak fault current is also reduced, see Fig. 13 (a). The fault energy is reduced by 18.5 % and 35.8 %. if single or multiple sequential DCCBs are used, see Fig. 13 (b). The fault current and energy on the adjacent line are shown in Fig. 13 (c-f). The $CB_{13}$ and $CB_{15}$ both operate in the current-limiting mode, they keep $i_{31}$ and $i_{51}$ constant. As these two adjacent lines are forced not over the DC current reference, the fluctuation is reduced, and system can restore faster.

The active power and average capacitor voltage of MMC1 are shown in Fig. 13 (g-h). The coordination control result in a smaller fluctuation, and the system recovery time is reduced by around 40 ms compared to the single conventional DCCB case. If make a comparison between Fig. 10, Fig. 11, and Fig. 13, it is observed that the single DCCB seldom has impact on the recovery process, but the proposed coordination method will significantly accelerate the process. Moreover, the proposed method shows a better performance in the seven-terminal DC grid, indicating that the proposed method is more suitable for future multi-link DC grid application.

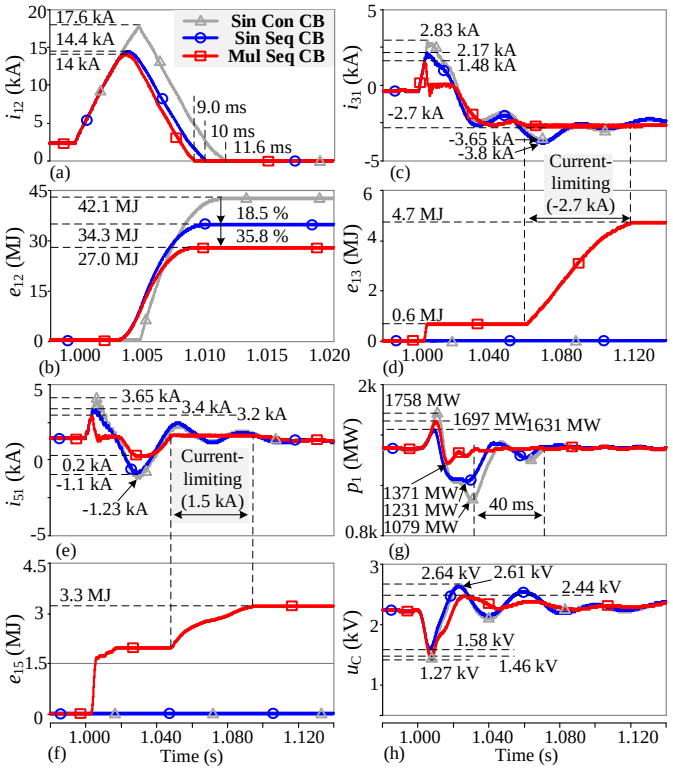


Fig. 13. Comparison of the fault interruption performance. (a) faulty line current; (b) faulty line DCCB energy; (c) adjacent line31 current; (d) adjacent line13 DCCB energy; (e) adjacent line51 current; (f) adjacent line15 DCCB energy; (g) MMC1 output power; (h) MMC1 capacitor voltages.

b) *Fault interruption performance of reclosing protection*

The pole-to-pole fault reclosing performance of the coordination method is verified in the seven-terminal system. The reclosing signal is given at t = 1.3 s. After a 2 ms relay delay, the second-time blocking signal is given to the faulty line DCCB.

As shown in Fig. 14 (a), the peak fault current of the original reclosing method will increase to 7.3 kA within 2 ms. The current of the coordination method only reaches to 2.5 kA because the $CB_{12}$ is operating in the current limiting mode after reclosed. The dissipated energy of $CB_{12}$ will reach to 51.5 MJ in the original method, but the energy is 29.9 MJ with the proposed coordination method, as shown in Fig. 14 (b). It is noted that the dissipated energy of the coordination method is even less than the energy in the primary protection of single conventional DCCB, and the total dissipated energy further reduced by 41.9 % when the reclosing process is considered.

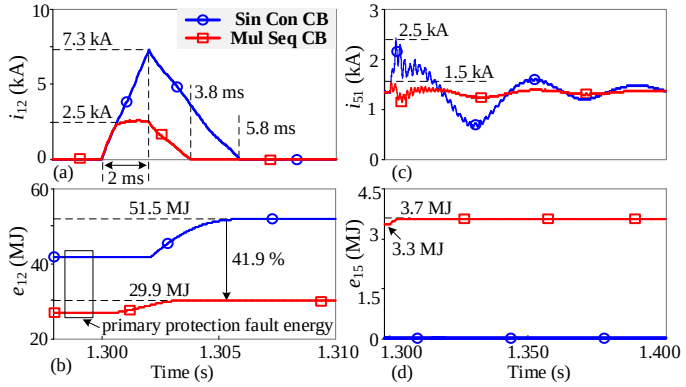


Fig. 14 Comparison of reclosing performance of the single conventional DCCB and multiple sequential DCCBs. (a) faulty line current; (b) faulty line DCCB energy; (c) adjacent line current; (d) adjacent line DCCB energy.

According to the flow before reclosing, $i_{13}$ will not reverse in such a short time. Thus, only $CB_{15}$ can participate in the current limiting. Therefore, only the current of $CB_{15}$ is shown in Fig. 14 (c). The current of coordination control is limited to 1.5 kA and the current will reach to 2.5 kA without involving $CB_{15}$. Moreover, the current fluctuation of $i_{51}$ is much smaller with the help of $CB_{15}$. The dissipated energy of $CB_{15}$ only increases 0.4 MJ compared to the primary protection, as shown in Fig. 14 (d). The results show that the coordination method can also reduce the peak current and dissipated energy in the reclosing process. The additional fault energy only increases a little and the disturbance to the DC grid is much lower.

## V. Economic Comparison and Discussion

The proposed method is compared to other DCCBs in protection performance, economic cost, and industrial feasibility. The comparison is between three types of DCCBs: 1) single conventional DCCB [10], 2) integrated DCCB [23], and 3) the proposed coordination of multiple sequential DCCBs.

The conventional DCCB use one individual DCCB to protect each line, and the integrated DCCB use one high voltage valve to protect all connected line. However, the conventional DCCB and integrated DCCB both block their main breaker totally after the current commutation process, so they have the same system fault response.

The coordination of multiple sequential DCCB can achieve a better protection performance by enhancing the controllability of conventional DCCB. The proposed method can reduce the peak fault current, dissipated energy, and recovery times of DC system, which is not discussed in the other methods. Taking the seven-terminal DC grid as an example, three protection methods' fault response are listed in Table II.

TABLE II
Fault Stress of Different DCCB

| protection methods | Sin Con DCCB | integrated DCCB | Mul Seq DCCB |
|---|---|---|---|
| primary peak current / kA | 17.6 | 17.6 | 14 |
| primary fault energy / MJ | 42.1 | 42.1 | 27 |
| secondary peak current / kA | 7.3 | 7.3 | 2.5 |
| secondary fault energy / MJ | 44.5 | 44.5 | 29.9 |
| recovery time / ms | 75 | 75 | 35 |

The proposed method can limit the fault current and dissipated energy during the fault, which means the system will suffer less disturbance, and the cost of one DCCB is reduced. The requirements for the IGBTs under different protection methods are discussed. IGBTs can achieve a high turnoff current by applying high gate-emitter voltage [27]. It will be mainly threatened by overheating when turning off a large current, and the IGBT's junction temperature ($T_{vj}$) can be calculated by its power loss and thermal module [28]. Taking the conventional protection method or coordination method in the seven-terminal DC grid as an example (Fig. 13 (a)), the junction temperature of ABB's 4.5kV/ 3kA IGBT [29] and 4.5kV / 2kA IGBT [30] are compared, as shown in Fig. 15.

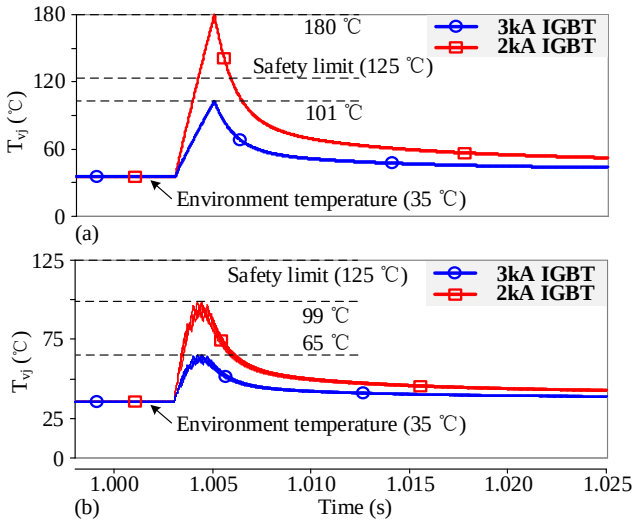


Fig. 15 Junction Temperature of main breaker IGBTs under (a) single conventional DCCB; (b) coordination method of multiple sequential DCCBs.

In the conventional method, a 3 kA IGBT can turn off 17.6 kA fault current with its junction temperature reaches 101 ℃, but a 2 kA IGBT will reach 180 ℃, see Fig. 15 (a). The temperature of 2 kA IGBT will exceed the safety limit of 125 ℃, so it is not satisfied in the conventional protection method. In the coordination method, the junction temperature reaches 65 ℃ for 3 kA IGBT, the temperature of 8 subunits of 2 kA IGBT reaches 99 ℃, respectively. Therefore, the 2 kA IGBT can satisfy the protection requirements, and 3 kA IGBT is unnecessary.

The proposed coordination method can reduce the requirements for large current IGBTs, but the cost of integrated DCCB is the cheapest as it only uses one high voltage valve to protect multiple lines. However, it also has some drawbacks compared to individual DCCBs. The integrated DCCB relies on

many LCSs and UFDs to ensure the fault current on every line flow through one high voltage valve, but individual DCCBs have their own corresponding LCS and UFD. The used UFDs and LCSs are shown in Table III, in which *n* is the number of lines connected to the DC bus.

Table. III
ECONOMIC EFFICIENCY COMPARISON

| protection methods | Sin Con DCCB | integrated DCCB | Mul Seq DCCB |
|---|---|---|---|
| Number of DCCB | *n* | 1 | *n* |
| Number of UFDs and LCSs | *n* | 2*n*+2 | *n* |
| Triggered number of UFDs and LCSs during one fault | 1 | *n*+1 | *n* |
| Near backup protection? | yes | no | yes |

The integrated DCCB needs more LCSs and UFDs in one breaker, and half of the LCSs and UFDs are used to build the commutation circuit during fault. The single DCCB method only triggers the faulty line DCCB to isolate the fault, and the proposed coordination method will trigger all near DCCBs. However, the integrated DCCB needs a complex structure design to connect multiple lines in one DCCB, but the individual DCCB only needs one input and one output line. The success of integrated DCCB relies on every UFD and LCS's acerate operation, and it lacks near end backup protection capability. The proposed coordination method has a simple current commutation process for each DCCB, and the near DCCBs can achieve backup protection.

The coordination method of DCCB can be achieved by software upgrades from the existing single DCCBs. The IGBT's control board can already measure current and voltage on every sub-module, but the signal interconnection between DCCBs need more devices. When the proposed method is upgraded from the existing DCCBs, it will have more reliability than the integrated DCCB. The system still has enough capability for backup protection even if one DCCB fails.

## VI. CONCLUSION

In this paper, coordination methods of multiple DCCBs are proposed to protect the HVDC grid, the fault energy is shared and the system recovery speed is increased. The control methods for primary/backup protection and reclosing logic is discussed. The coordination of sequential DCCBs is preferred due to is has better controllability than single DCCBs.

The proposed coordination method enhanced the controllability of multiple DCCBs, so the effect will better than single DCCB protection, and it is verified in the Zhangbei system. For example, the energy dissipation requirement is reduced by 30.5-41.9 %, and the fault recovery time is reduced by 20-40 ms. Compared with a four-terminal DC grid, the proposed method achieves better results in a seven-terminal DC grid. This indicates that the proposed method has better applicability for a HVDC grid with more links connected to one DC bus.

The proposed method's effect relies on the correct operation of all DCCBs, a failure operation of one certain DCCB may cause reduce the protection effect of the proposed method. The trigger signal transmission from the faulty line DCCB to adjacent DCCBs also impacts the protection effect, a fast and reliable signal transmission is needed to activate proper coordination protection.

It should also be highlighted that an experimental validation of the proposed protection scheme, although highly desirable to verify its performance, falls out of the scope of this work. However, the experimental verification of the single sequential DCCB has been shown in [19]. Therefore, a better protection performance of multiple DCCBs can be expected in the meshed DC grid.

## REFERENCES


[1] N. Flourentzou, V. G. Agelidis and G. D. Demetriades, "VSC-Based HVDC Power Transmission Systems: An Overview," *IEEE Trans. Power Electron*, vol. 24, no. 3, pp. 592-602, March 2009.

[2] D. Van Hertem and M. Ghandhari, "Multi-terminal VSC HVdc for the European Supergrid: Obstacles," *Renew. Sustain. Energy Rev*, vol. 14, no. 9, pp. 3156–3163, 2010

[3] T. An, G. Tang, and W. Wang, "Research and application on multiterminal and DC grids based on VSC-HVDC technology in China," IET High Voltage, vol.2, no.1, pp.1-10, 2017.

[4] X. Han, W. Sima, M. Yang, L. Li, T. Yuan and Y. Si, "Transient Characteristics Under Ground and Short-Circuit Faults in a ±500 kV MMC-Based HVDC System with Hybrid DC Circuit Breakers," *IEEE Trans. Power Deliv*, vol. 33, no. 3, pp. 1378-1387, June 2018.

[5] S. Li, J. Xu, Y. Lu, C Zhao, J Zhang, C Jiang and S Qiu, "An Auxiliary DC Circuit Breaker Utilizing an Augmented MMC," *IEEE Trans Power Deliv*, vol. 34, no. 2, pp. 561-571, April 2019.

[6] J. Xu, X. Zhao, H. Jing, J. Liang and C. Zhao, "DC Fault Current Clearance at the Source Side of HVDC Grid Using Hybrid MMC," *IEEE Trans. Power Deliv*, vol. 35, no. 1, pp. 140-149, Feb. 2020.

[7] W. Lin, D. Jovcic, S. Nguefeu and H. Saad, "Full-Bridge MMC Converter Optimal Design to HVDC Operational Requirements," *IEEE Transactions on Power Delivery*, vol. 31, no. 3, pp. 1342-1350, June 2016.

[8] Q. Song X. Li W. Yang et al., "A Modular Multilevel Converter Integrated with DC Circuit Breaker," *IEEE Trans. Power Deliv*, vol. 33, no. 5, pp. 2502-2512, Oct. 2018.

[9] S. Wang, C. Li, O. D. Adeuyi, G. Li, C. E. Ugalde-Loo and J. Liang, "Coordination of MMCs With Hybrid DC Circuit Breakers for HVDC Grid Protection," *IEEE Trans. Power Deliv*, vol. 34, pp. 11-22, Feb. 2019.

[10] A. Hassanpoor, J. Häfner and B. Jacobson, "Technical Assessment of Load Commutation Switch in Hybrid HVDC Breaker," *IEEE Trans. Power Electron*, vol.30, no.10, pp.5393-5400, Oct. 2015.

[11] G. Tang, Z. He, H. Pang, X. Huang and X. Zhang, "Basic topology and key devices of the five-terminal DC grid," *CSEE Journal of Power and Energy Systems*, vol. 1, no. 2, pp. 22-35, June 2015

[12] G Tang, H. Pang and X. Wei, "Research on Key Technology and Equipment for Zhangbei 500kV DC Grid," *2018 Inter Power Electron Con (IPEC)*, Niigata, 2018, pp. 2343-2351

[13] D. Jovcic, G. Tang and H. Pang, "Adopting Circuit Breakers for HighVoltage dc Networks: Appropriating the Vast Advantages of dc Transmission Grids," *IEEE Power Energy Mag*, vol. 17, no. 3, pp. 82-93, May-June 2019.

[14] R. Majumder, *et al.*, "An Alternative Method to Build dc Switchyard with Hybrid DC breaker for dc grid", *IEEE Trans. Power Deliv.*, vol. 32, no. 2, pp. 713-722, April. 2017.

[15] B. Li, J. He, Y. Li, W. Wen and B. Li, "A Novel Current- Commutation-Based FCL for the Flexible DC Grid," *IEEE Trans. on Power Electron*, vol. 35, no. 1, pp. 591-606, Jan. 2020.

[16] Y. Guo, G. Wang, D. Zeng, H. Li and H. Chao, "A Thyristor Full-Bridge-Based DC Circuit Breaker," *IEEE Trans. on Power Electron*, vol. 35, no. 1, pp. 1111-1123, Jan. 2020

[17] A. Jamshidi Far and D. Jovcic, "Design, Modeling and Control of Hybrid DC Circuit Breaker Based on Fast Thyristors," *IEEE Trans. Power Deliv*, vol. 33, no. 2, pp. 919-927, April 2018.

[18] Y. Song, J Sun, M Saeedifard, S Ji, L Zhu, and L Graber., "Reducing the Fault-Transient Magnitudes in Multiterminal HVdc Grids by Sequential Tripping of Hybrid Circuit Breaker Modules," *IEEE Trans. Ind. Electron*, vol. 66, no. 9, pp. 7290-7299, Sept. 2019.

[19] M. H. Hedayati and D. Jovcic, "Reducing Peak Current and Energy Dissipation in Hybrid HVDC CBs Using Disconnector Voltage Control," *IEEE Trans. on Power Deliv*, vol. 33, no. 4, pp. 2030-2038, Aug. 2018.
[20] G. Liu, F. Xu, Z. Xu, Z. Zhang and G. Tang, "Assembly HVDC Breaker for HVDC Grids with Modular Multilevel Converters," *IEEE Trans. Power Electron*, vol. 32, no. 2, pp. 931-941, Feb. 2017.
[21] C. Li, J. Liang and S. Wang, "Interlink Hybrid DC Circuit Breaker," *IEEE Trans. Ind Electron*, vol. 65, no. 11, pp. 8677-8686, Nov. 2018.
[22] A. Mokhberdoran, D. Van Hertem, N. Silva, H. Leite and A. Carvalho, "Multiport Hybrid HVDC Circuit Breaker," *IEEE Trans. Ind. Electron.*, vol. 65, no. 1, pp. 309-320, Jan. 2018.
[23] E. Kontos, T. Schultz, L. Mackay, L. M. Ramirez-Elizondo, C. M. Franck and P. Bauer, "Multiline Breaker for HVdc Applications," *IEEE Trans. Power Deliv.*, vol. 33, no. 3, pp. 1469-1478, June 2018.
[24] W. Lin, D. Jovcic, S. Nguefeu, and H. Saad, "Modelling of high-power hybrid DC circuit breaker for grid-level studies", *IET Power Electron.* vol 9, no 2, pp 237-246, Jan. 2016.
[25] C. Li, C. Zhao, J. Xu, Y. Ji, F. Zhang and T. An, "A Pole-to-Pole ShortCircuit Fault Current Calculation Method for DC Grids," *IEEE Trans. Power Syst.*, vol. 32, no. 6, pp. 4943-4953, Nov. 2017.
[26] X. Guo, Y. Zhou, et al, "Research on the Fault Current Characteristic and Suppression Strategy of Zhangbei Project," *Proceedings of the CSEE*, vol. 38, no. 18, pp. 5438-5446, Sep. 2018 (in Chinese)
[27] Z. Chen, Z Yu, X, Zhang, *et al*., "Analysis and Experiments for IGBT, IEGT, and IGCT in Hybrid DC Circuit Breaker," *IEEE Trans. Ind Electron*, vol. 65, no. 4, pp. 2883-2892, April 2018.
[28] A. Jamshidi Far and D. Jovcic, *"*Design, Modeling and Control of Hybrid DC Circuit Breaker Based on Fast Thyristors*," IEEE Trans. Power Deliv*, vol. 33, no. 2, pp. 919-927, April 2018.
[29] "5SNA 3000K452300 data sheet", ABB, Nov 2017. www.hitachiabb-powergrids.com.
[30] "5SNA 2000K452300 data sheet", ABB, Oct 2016. www.hitachiabb-powergrids.com.

**Xibei Zhao** received the B.S degree in Electrical Engineering and Its Automation from Chongqing University (CQU) in 2015, currently he is a Ph.D. student in Electrical Engineering in North China Electric Power University (NCEPU) from 2017. From Aug 2019 to Oct 2020, he is a joint Ph.D. student at Cardiff University. His research interests include HVDC grid operation and protection.

**Jianzhong Xu** (M'14) received the B.S. in Thermal Power and Its Automation and the Ph.D. degree in Electrical Engineering from North China Electric Power University (NCEPU), Beijing, China, in 2009 and 2014, respectively. From 2012 to 2013 and 2016 to 2017, he was, respectively, a joint Ph.D. student and Postdoctoral Fellow with the University of Manitoba. He is currently an Associate Professor with the State Key Laboratory of Alternate Electrical Power System with Renewable Energy Sources, NCEPU. His research interests include the high-speed electromagnetic transient modeling, control, and protection of MMC-HVdc and DC grid.

**Gen Li** (M'18) received his B.Eng. degree in Electrical Engineering and its Automation from Northeast Electric Power University, Jilin, China, in 2011, his M.Sc. degree in Power Engineering from Nanyang Technological University, Singapore, in 2013 and his Ph.D. degree in Electrical Engineering from Cardiff University, Cardiff, U.K., in 2018.

From 2013 to 2016, he was a Marie Curie Early Stage Research Fellow funded by the European Union's MEDOW project. He has been a Visiting Researcher at China Electric Power Research Institute and Global Energy Interconnection Research Institute, Beijing, China, at Elia, Brussels, Belgium and at Toshiba International (Europe), London, U.K. He has been a Research Associate at the School of Engineering, Cardiff University since 2017. His research interests include control and protection of HVDC and MVDC technologies, power electronics, reliability modeling and evaluation of power electronics systems.

Dr. Li is a Chartered Engineer in the U.K. He is an Associate Editor of the CSEE Journal of Power and Energy Systems. He is an Editorial board member of CIGRE ELECTRA. His Ph.D. thesis received the First CIGRE Thesis Award in 2018.

**Jinsha Yuan** received the M.E. degree in theoretical electrical engineering and the Ph.D. degree in electrical engineering and its automation from North China Electric Power College, Baoding, China, in 1987 and 1992, respectively. He is currently a Professor and a Ph.D. Supervisor with North China Electric Power University, Baoding. His research interests include intelligent information processing technology, wireless communication, and electromagnetic field numerical calculation method and application.

**Jun Liang** received the B.Sc. degree from Huazhong University of Science and Technology, Wuhan, China, in 1992 and the M.Sc. and Ph.D. degrees from the China Electric Power Research Institute (CEPRI), Beijing, in 1995 and 1998, respectively. From 1998 to 2001, he was a Senior Engineer with CEPRI. From 2001 to 2005, he was a Research Associate with Imperial College London, U.K.. From 2005 to 2007, he was with the University of Glamorgan as a Senior Lecturer. Currently, he is a Professor at the School of Engineering, Cardiff University, Cardiff, U.K.. He is a Fellow of the Institution of Engineering and Technology (IET). He is the Chair of IEEE UK and Ireland Power Electronics Chapter. He is an Editorial Board Member of CSEE JPES. He is the Coordinator and Scientist-in-Charge of two EC Marie-Curie Action ITN/ETN projects: MEDOW (€3.9M) and InnoDC (€3.9M). His research interests include HVDC, MVDC, FACTS, power system stability control, power electronics, and renewable power generation.

**Chongru Liu** received her B.S., M.S. and Ph.D. in E.E. from Tsinghua University, Beijing, China. She was a visiting professor at the University of Hong Kong from 2009 to 2010, and she was a visiting professor at Washington State University from 2010 to 2011. She is currently a professor in the School of Electrical and Electronic Engineering, North China Electric Power University. Dr. Liu is a member of the National Power System Management and Information Exchange Standardization Committee of China. She is a member of Beijing Nova and supported by the program of New Century Excellent Talents in University.